Christopher Tsai
February 22, 2008
EE 262 – 2D Imaging

Problem Set VII – Rotational Symmetry

Problem #2 – Telescope Response

(a.) A round telescope aperture, if modeled ideally as a circ function, will produce an intensity response that resembles a scaled squared jinc function, which we normalize and image below:

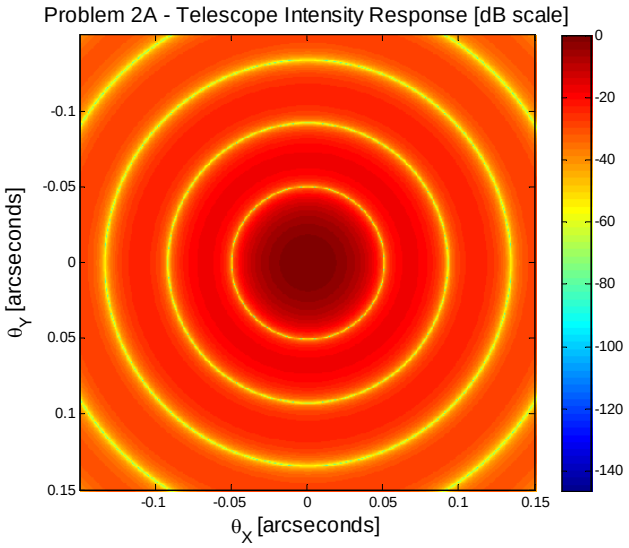

We plot a normalized one-dimensional cross-section through the center of the intensity response:

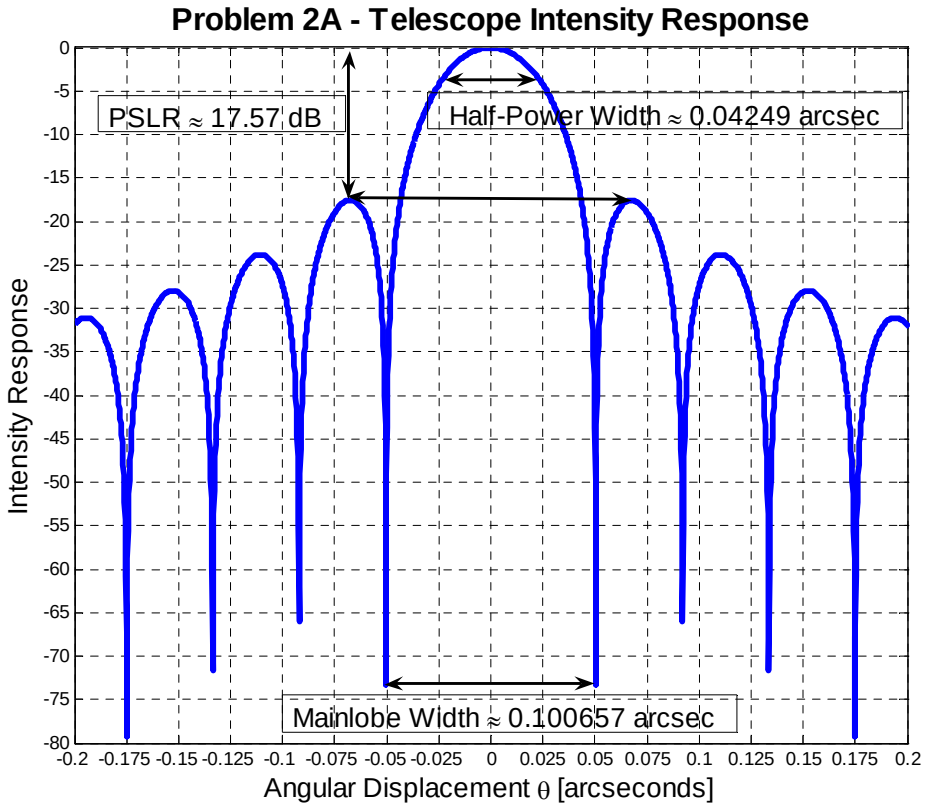

The null-to-null main lobe width appears to be 0.100657 seconds of arc. As expected, the response behaves like a squared jinc pattern, with sidelobes decaying at an inverse square rate.

(b.) The two-dimensional intensity response has a series of light rings surrounding the central peak; in our one-dimensional cross-section, these rings appear as sidelobes protruding on either side of the main lobe. The ratio of intensities of the main lobe to the first side lobe is approximately 17.570153 decibels, or roughly 18 dB.

(c.) For rectangular apertures, a cosine weighting reduces sidelobe levels; we can apply a similar aperture tapering technique here for circular windows to suppress the sidelobes of our Bessel function. We choose the following cosine aperture, scaling our Bessel function so that the edges of the aperture coincide with the shifted Bessel function global minimum:

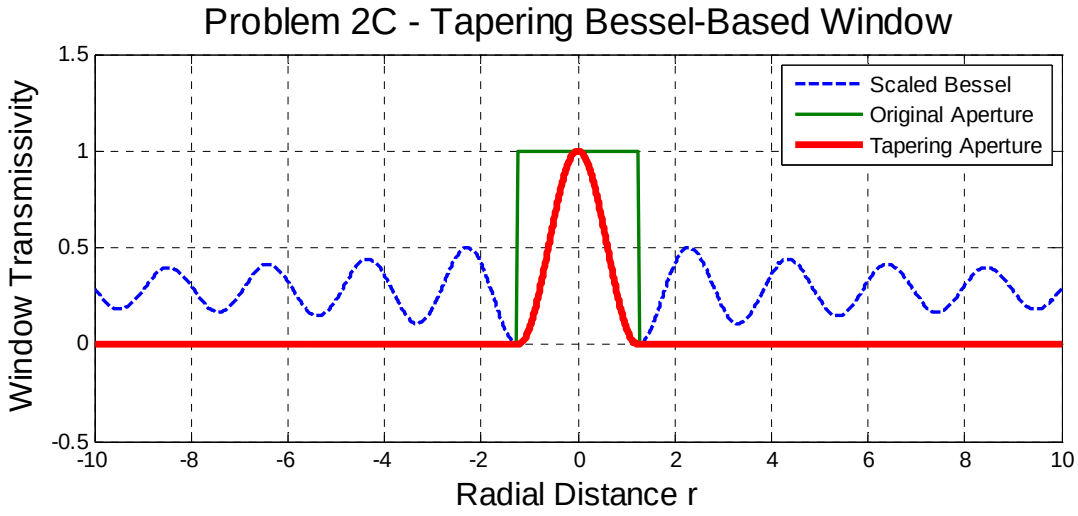

To measure the effect in the Fraunhofer intensity regime, we transform the weighted circ aperture and study a one-dimensional cross-section yet again. First, however, we plot the two-dimensional spectrum for perspective:

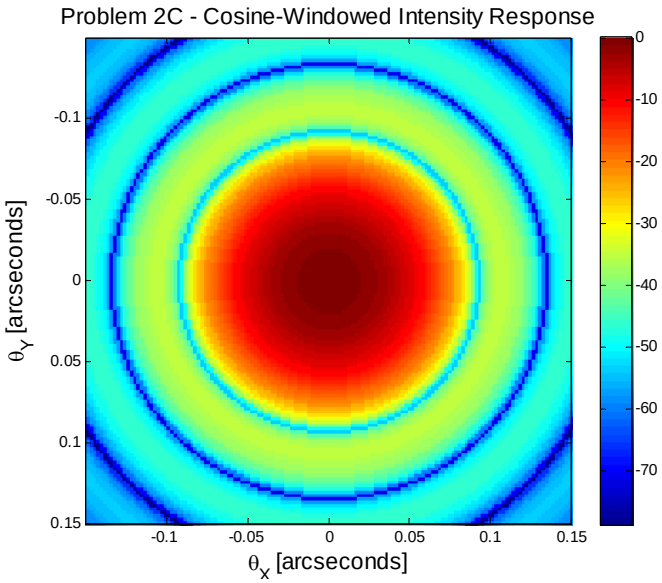

As the plot on the following page reveals, the tapering widens the main lobe and suppresses the side lobes. Thus, although smearing the aperture has increased the amount of higher-frequency content in the main lobe, the tapering effect also moderates the sidelobe height.

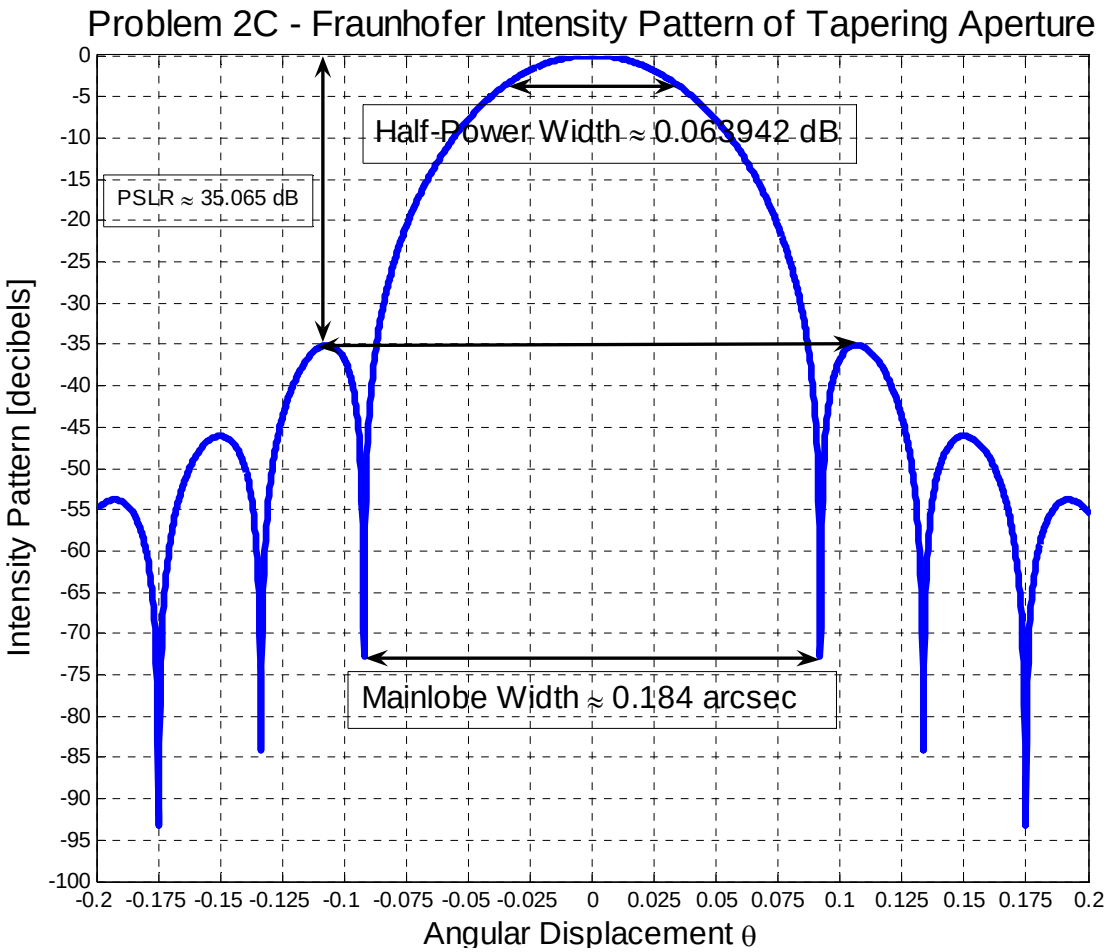

One drawback to our tapered aperture is its wider main lobe; the width has increased from 0.100657 arcsecond to 0.183988 arcseconds, thereby compromising the pinpoint precision of our telescope. However, the new peak sidelobe ratio (PSLR) of the weighted aperture is approximately 35.065181 dB, nearly twice the PSLR for the unweighted case, reassuring us that our window has significantly attenuated sidelobes.

Sidelobe suppression is integral to detecting weaker stellar companion stars because it prevents adjacent amplification or sidelobe replication of stronger neighboring mainstream stars from overpowering and dissembling the presence of the weak companion star; sidelobes serve (to first order) as shifted impulses, generating replicas of nearby objects that potentially interfere with the image extracted by the main lobe. Without sidelobe reduction, these stronger stars might generate a sidelobe echo that is greater than an interstellar weaker star's main lobe, thus concealing or even belying the presence of the weaker stellar companion star. By suppressing the sidelobes, we reduce the response of neighboring stars, preventing a strong nearby star from interfering and overwhelming the signal from the weak star we are trying to image.

(d.) We can determine the half-power widths of our intensity patterns from the cross-sections plotted previously. The ideal aperture yielded a power pattern with half-power width of approximately 0.042491 arcseconds, whereas our tapered aperture broadens this width to around 0.063942 arcseconds! All in all, windowing the sharp circ aperture widens the main lobe but more than doubles the PSLR measured in decibel scale! This sidelobe suppression more than atones for the loss in central locality.

Problem #3 – Fourier Transforms vs. Hankel Transforms

The Hankel transform of a circularly symmetric function is a one-dimensional representation of the two-dimensional Fourier transform. Let us compare the numerical results of the Hankel transform of a rect function using the integral definition of the Hankel transform against using a two-dimensional Fourier transform. We define our rect function as

$$f(r) = \frac{4}{\pi a^2}\Pi\left(\frac{r}{a}\right)$$

The Hankel transform of this function should assume the analytical form:

$$\mathcal{H}\{f(r)\} = \frac{4}{\pi} jinc(aq)$$

We let n be the first power of 2 greater than $4a$.

(a.) Setting $a = 32$, we sample $f(r)$ at $r = 0, 1, 2, \ldots, n-1$. For $a = 32$, $n = 256$. We numerically compute the Hankel transform with

```
function F = HankelTransform (f, dr, q)

% Discretizing the spatial domain:
r = (0.001 : dr : 100).';

% Discretizing the Hankel integral and evaluating for each frequency q:
F = sum(2*pi* repmat(feval(f,r).*r,1,length(q)) .* besselj(0,2*pi*r*q), 1);
F = F * dr;
```

The Hankel transform of our discretely sampled function closely resembles the Bessel function we suspect:

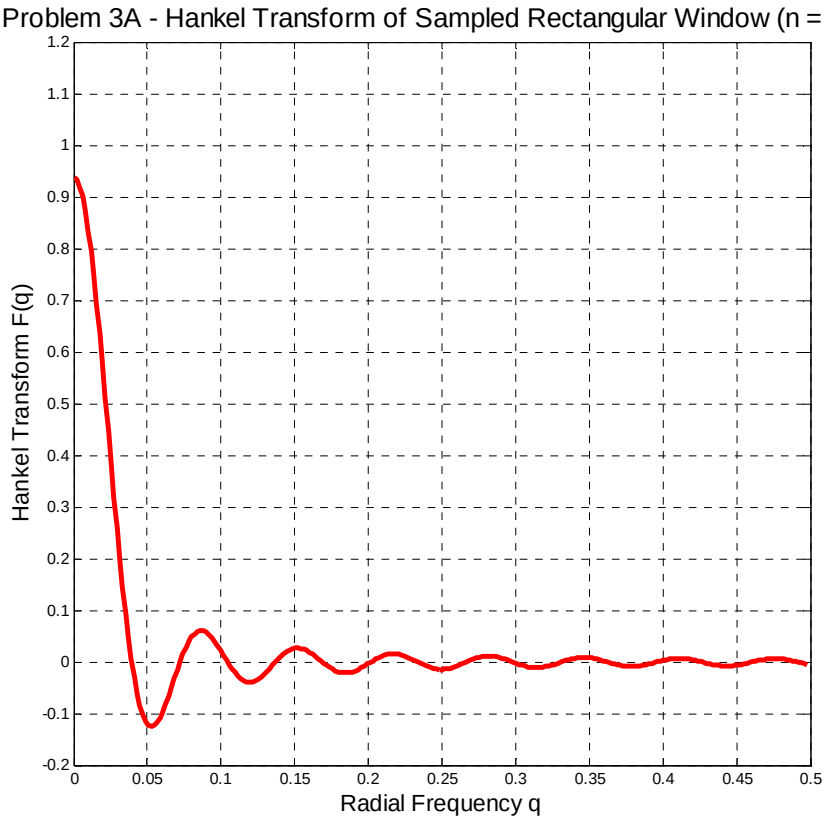

(b.) We now consider the circularly symmetric rectangle function as a circ function:

$$f(r) = \frac{4}{\pi a^2}\,\mathrm{circ}\left(\frac{2r}{a}\right) = \frac{4}{\pi a^2}\,\mathrm{circ}\left(\frac{2\sqrt{x^2+y^2}}{a}\right)$$

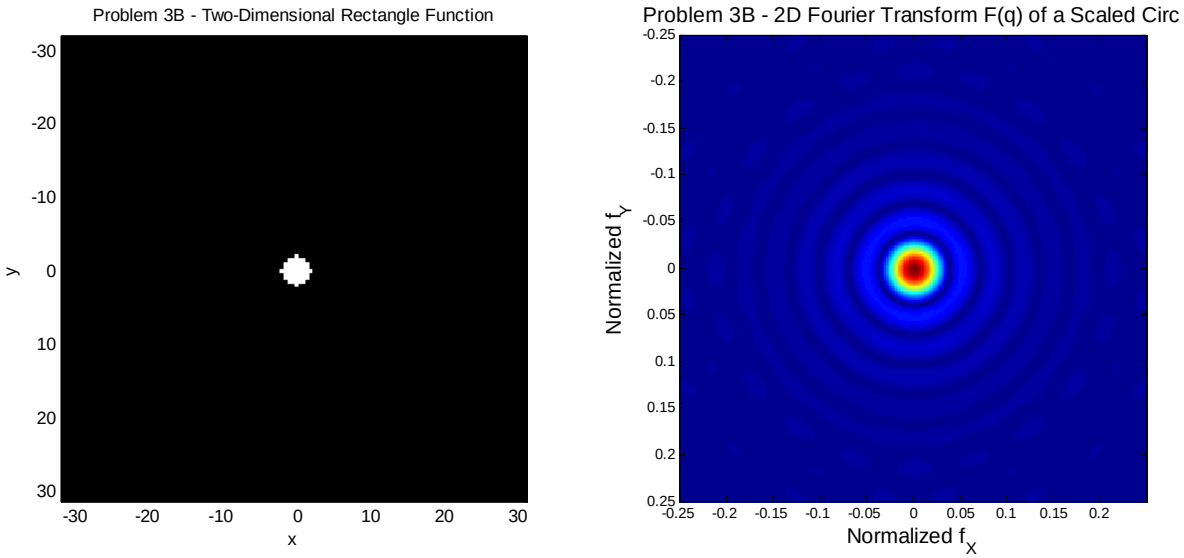

The magnitude spectrum resembles our original one-dimensional Bessel function along every single slice, so we have an azimuthally symmetric Bessel function, or *jinc*. Along each one-

dimensional slice, we can verify that the two-dimensional spectrum is, indeed, a fully rotated version of the Bessel function:

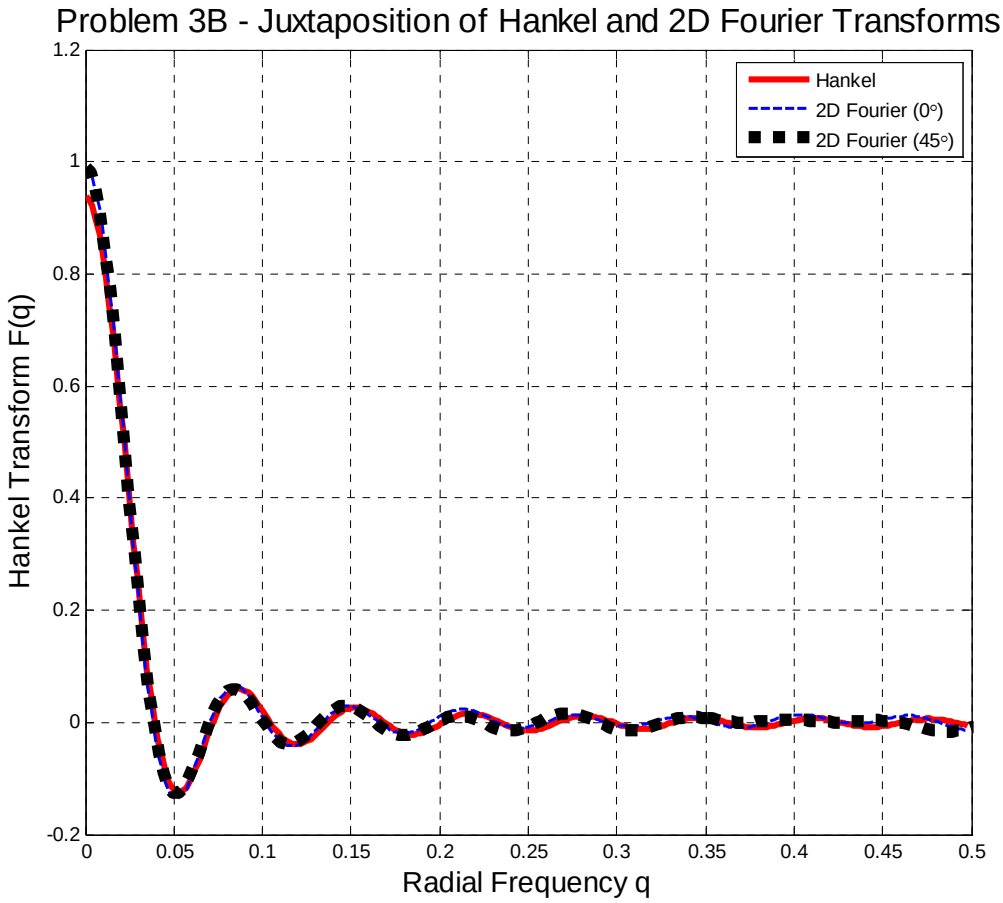

Indeed, the numerical Hankel transform computed in the previous part closely matches the two-dimensional Fourier transform sliced along both the horizontal and diagonal axes. We attribute the slight discrepancy to discretization differences, but, for all practical purposes, the functions closely match when we properly scale the axes (by $\sqrt{2}$ along the line $f_Y = f_X$).

(c.) We plot the analytical transform

$$\mathcal{H}\{f(r)\} = \frac{4}{\pi} jinc(aq)$$

on the same plot and ascertain that the three plots agree.

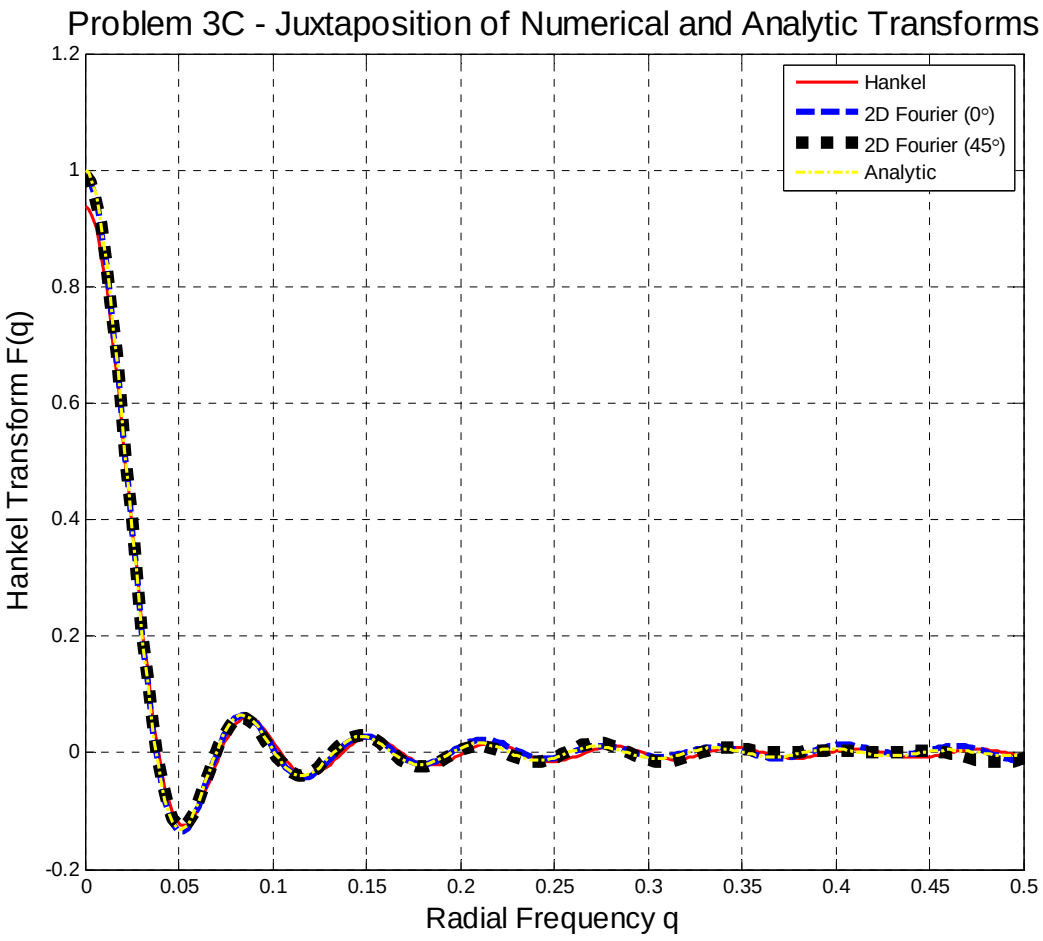

Differing discretization slightly differentiates the analytic and numeric transforms, but our sampling is fine enough to achieve a close match between the sampled analytic transform and numerically transformed samples; for $a = 32$, $n = 256$, so our sampling frequency comfortably exceeds the maximal sidelobes frequencies for the first few sidelobes, differing only at much higher (aliased) frequency sidelobes, whose amplitudes have such low relative value that we barely notice these higher-order discrepancies. All in all, the analytic transform accords with the two Fourier slices and the Hankel transform, with numerical discretization slightly degrading the higher-frequency content; however, for the most part, the discretization boasts short enough spacing that the frequency domain retains adequate resolution.

(d.) If we decrease a to 8, then $n = 64$, a factor of four smaller. With a lower parameter a and therefore fewer samples in space, the numerical transform representations no longer track one

another indistinguishably. The Hankel transform, in particular, suffers the most from the inadequate sampling, as it deviates the farthest from the analytic solution. Meanwhile, because the spectrum has widened, we encounter much more fringe aliasing, resulting in slightly heightened sidelobes:

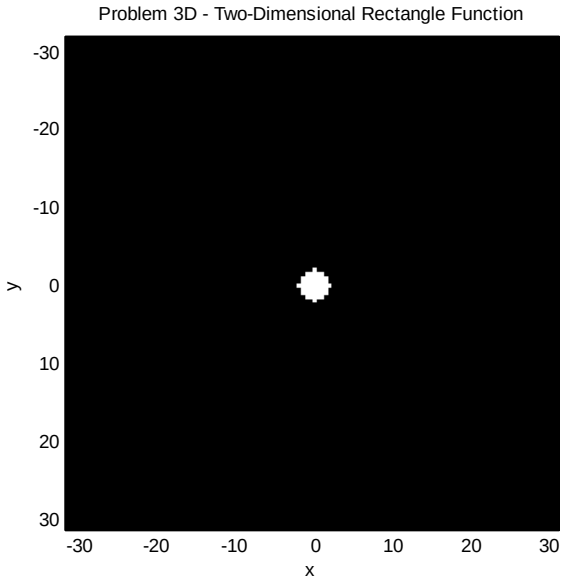

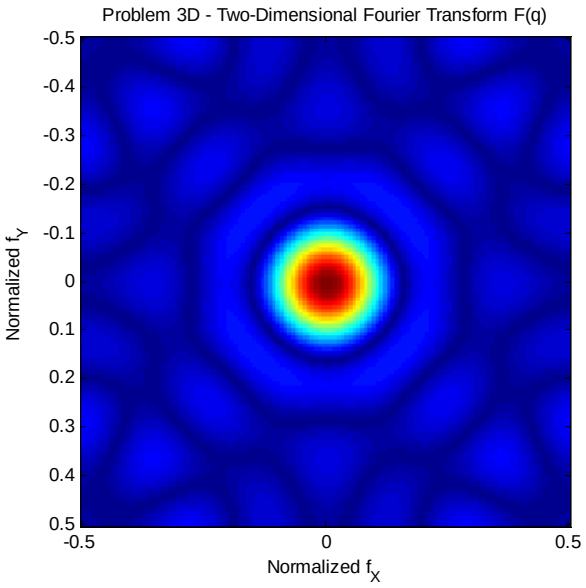

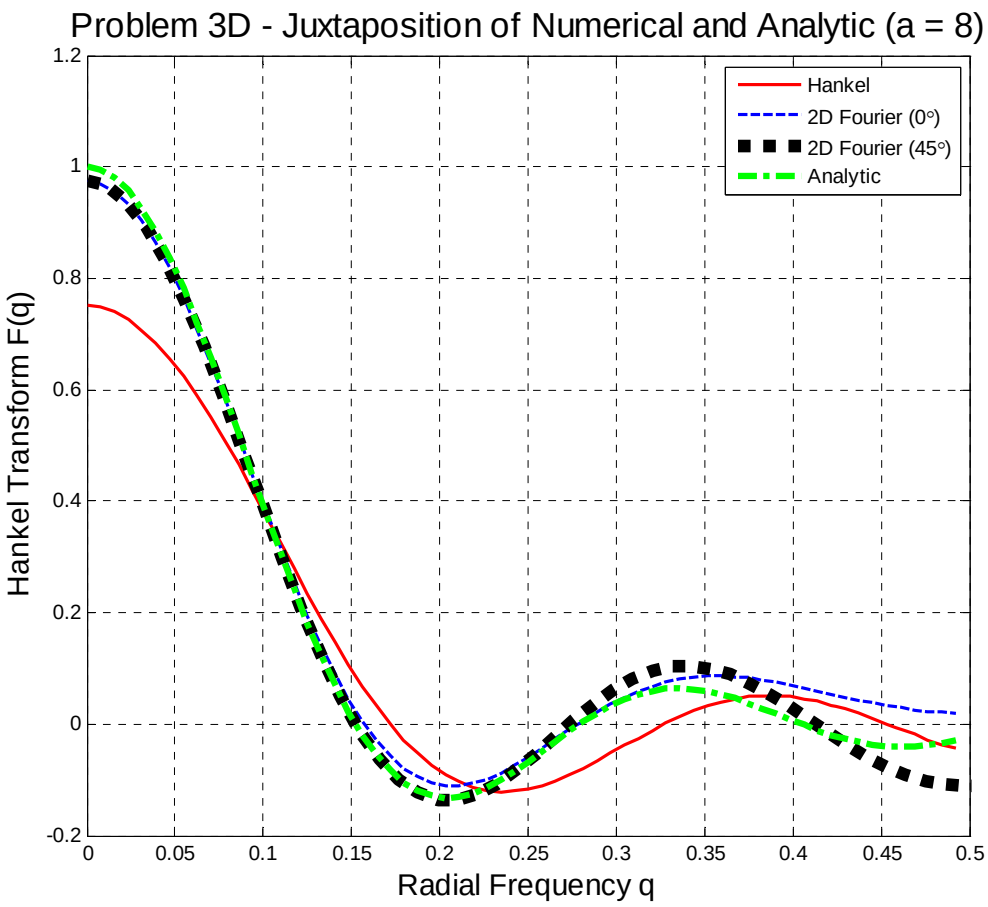

Problem #4 – Transform Inversion

The values given in hw7p4data represent a noisy projection of a circularly symmetric function as acquired by a tomographic scanner; in other words, the measured curve constitutes an Abel transform of the original object, which we now strive to recover. The data, as it appears on the disk, resembles a cosinusoid:

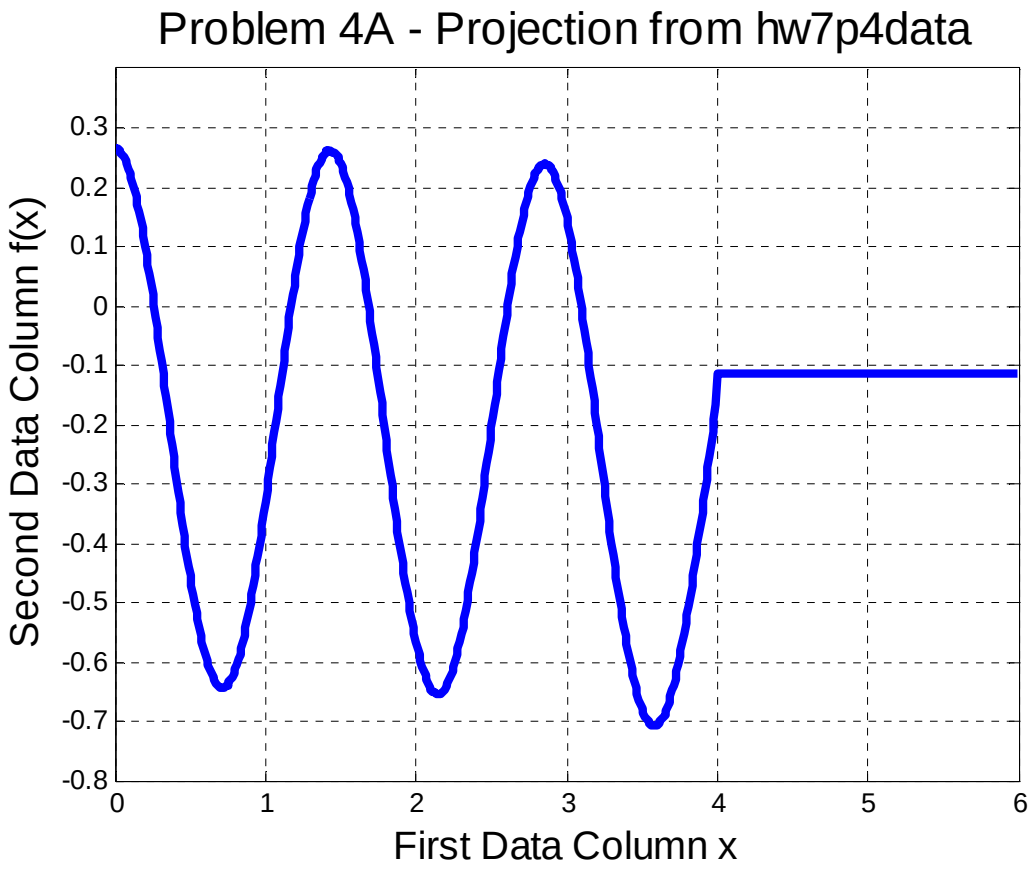

In order to recover the original function, we assume our signal to be an Abel transform and subsequently calculate its Fourier transform. A rotationally symmetric function possesses a Hankel transform that matches the one-dimensional Fourier transform of the function's Abel transform; in other words, performing a Fourier transform on a rotationally symmetric function's Abel transform is equivalent to Hankel transforming the function. Therefore, if we are to recover the function from its Abel transform, we can simply tap the inverse Hankel transform to recover the original signal, which we display to be jinc-like (Bessel-shaped) in our next plot:

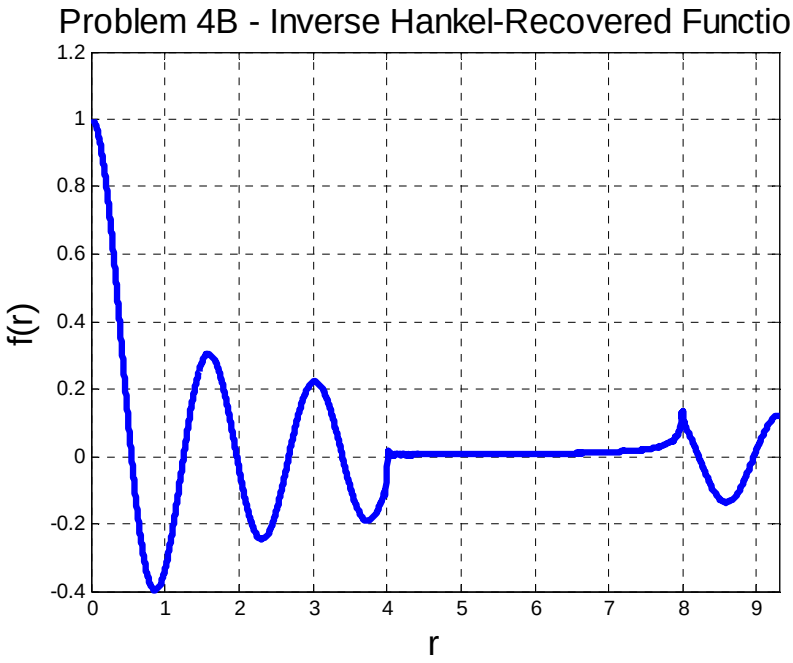

The transformed function is generally smooth, but we notice some spatial aliasing at the function's tail end, where a bit of irregular ripple disturbs the general stabilization. However, despite this perturbation, we can recover the original function by exploiting the function's predetermined rotational symmetry. In other words, we assume that the Abel transform data we receive is *even* and real-valued, so that we can restore $f(r)$ by mapping the function for $r > 0$ into a two-dimensional imaging plane. The image ascertains that the aforementioned tail plays a negligible role:

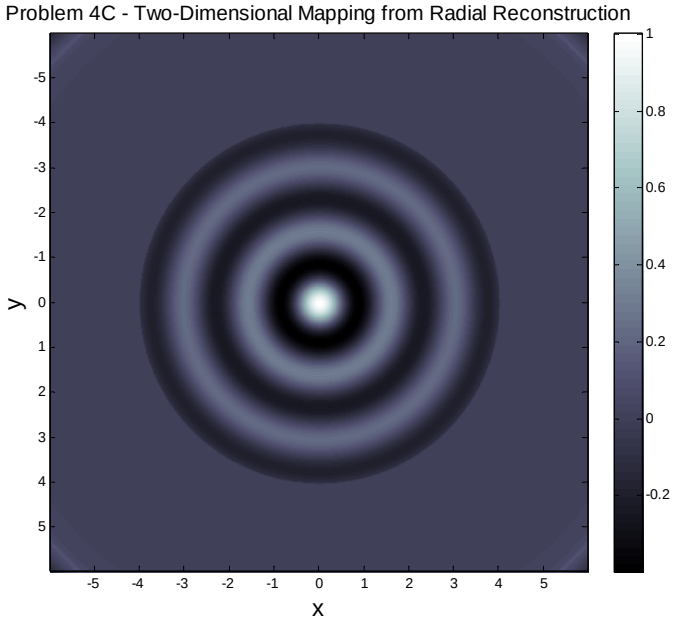

Problem #5 – Homemade Bessel

We rely on the integral definition of the zeroth-order Bessel function:

$$J_0(2\pi qr) = \frac{1}{2\pi}\int_0^{2\pi} \cos(2\pi qr\ \cos\theta)\ d\theta$$

Hence, we can manufacture zeroth-order Bessel functions of various frequencies by assembling a series of cosines. Each Bessel function also defines a circularly symmetric image, which we can view by rotating our one-dimensional Bessel function around a circle.

We produce Bessel functions at three frequencies: 4, 7, and 10 cycles over 1024 points. For each Bessel function we approximate, we also pirouette the one-dimensional slice to form a surface in $\mathbb{R}^3$. However, because we discretize the integral as a finite Riemann sum, we do not have cosines of every single frequency at our behest, so we can approximate the integral at best with a finite number of cosines with finely spaced frequencies. Consequently, our reconstruction will break down at higher frequencies, but we can choose this high frequency to be arbitrarily high, thereby matching the true Bessel function within a desired interval.

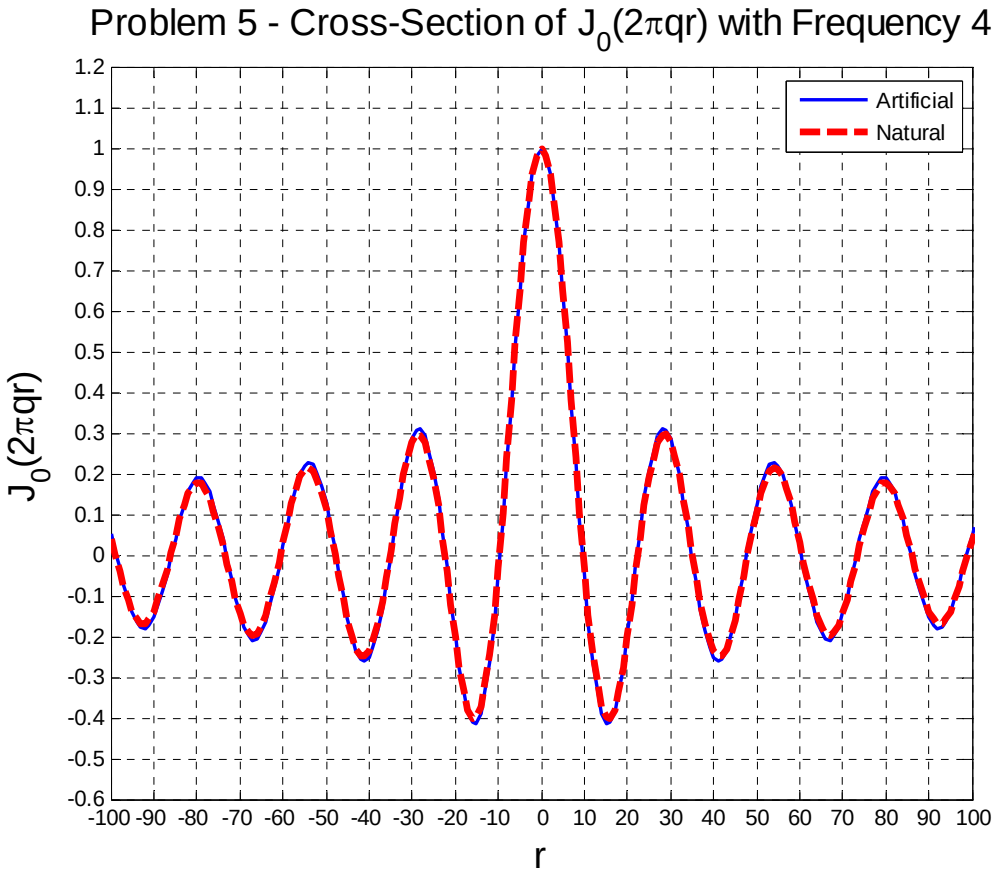
Problem 5 - Cross-Section of J0(2πqr) with Frequency 4
Artificial
Natural
J0(2πqr)
r
1.2
1.1
1
0.9
0.8
0.7
0.6
0.5
0.4
0.3
0.2
0.1
0
-0.1
-0.2
-0.3
-0.4
-0.5
-0.6
-100 -90 -80 -70 -60 -50 -40 -30 -20 -10 0 10 20 30 40 50 60 70 80 90 100

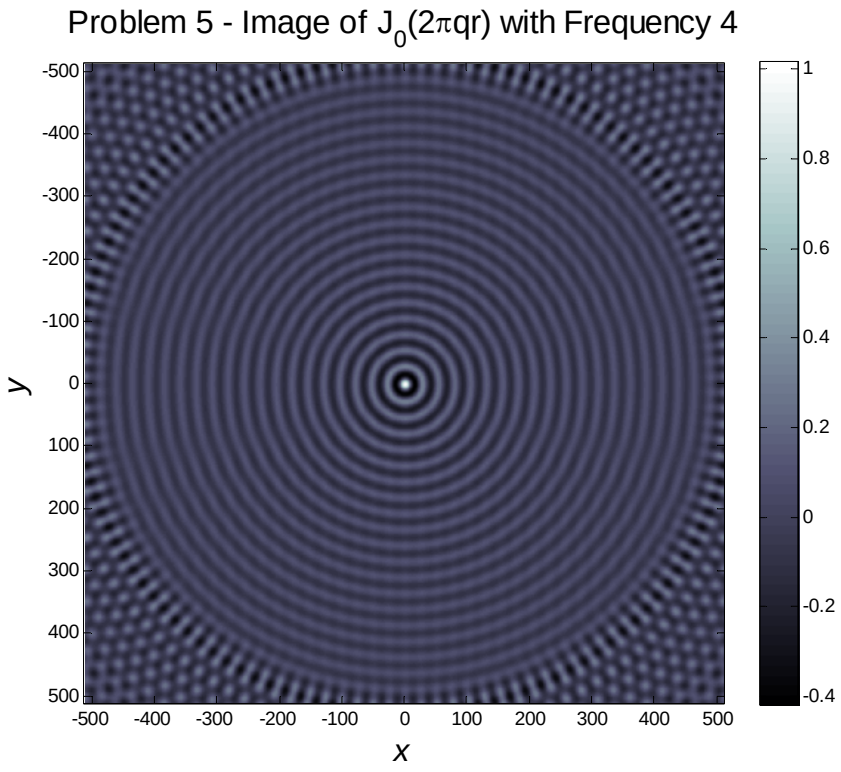
Problem 5 - Image of J0(2πqr) with Frequency 4
y
x
-500
-400
-300
-200
-100
0
100
200
300
400
500
1
0.8
0.6
0.4
0.2
0
-0.2
-0.4

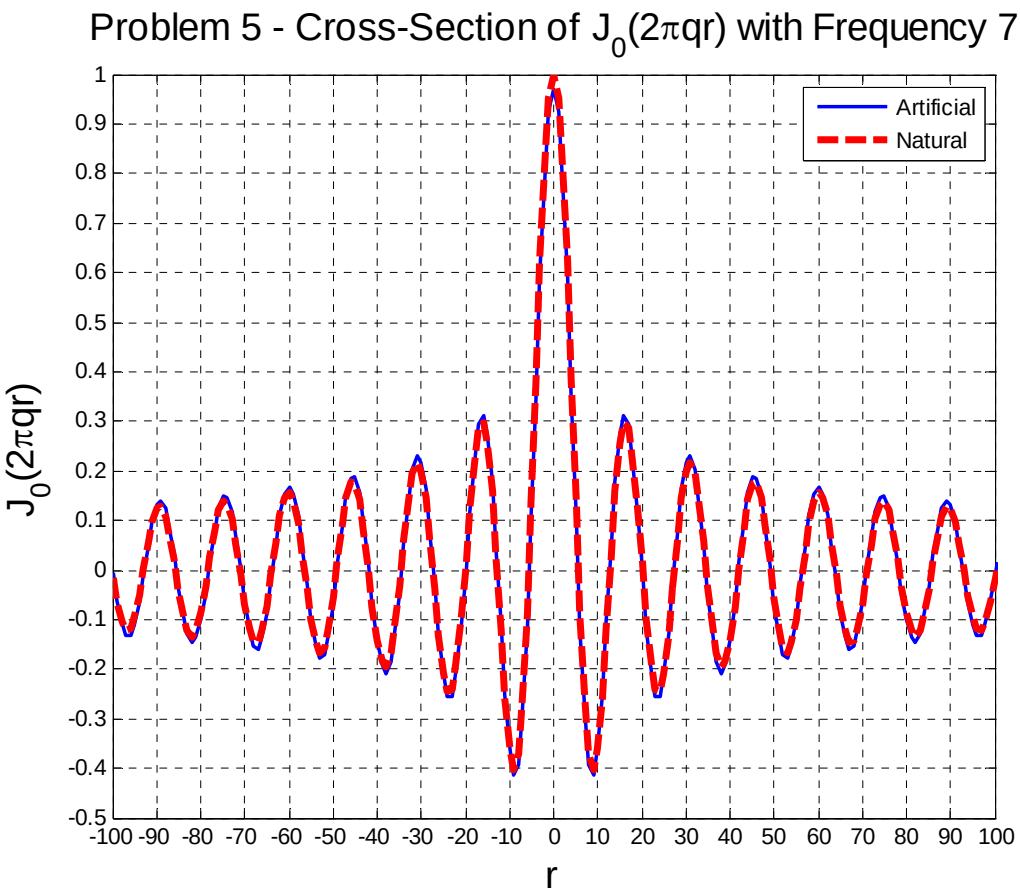
Problem 5 - Cross-Section of J0(2πqr) with Frequency 7
Artificial
Natural
J0(2πqr)
r
1
0.9
0.8
0.7
0.6
0.5
0.4
0.3
0.2
0.1
0
-0.1
-0.2
-0.3
-0.4
-0.5
-100 -90 -80 -70 -60 -50 -40 -30 -20 -10 0 10 20 30 40 50 60 70 80 90 100

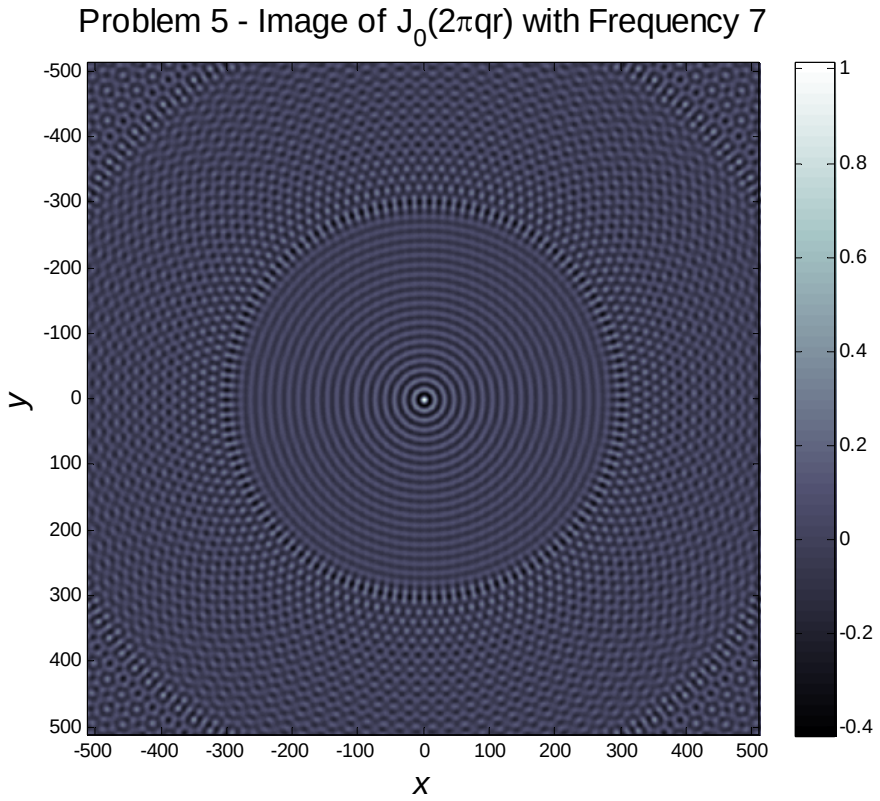
Problem 5 - Image of J0(2πqr) with Frequency 7
y
x
-500 -400 -300 -200 -100 0 100 200 300 400 500
1
0.8
0.6
0.4
0.2
0
-0.2
-0.4

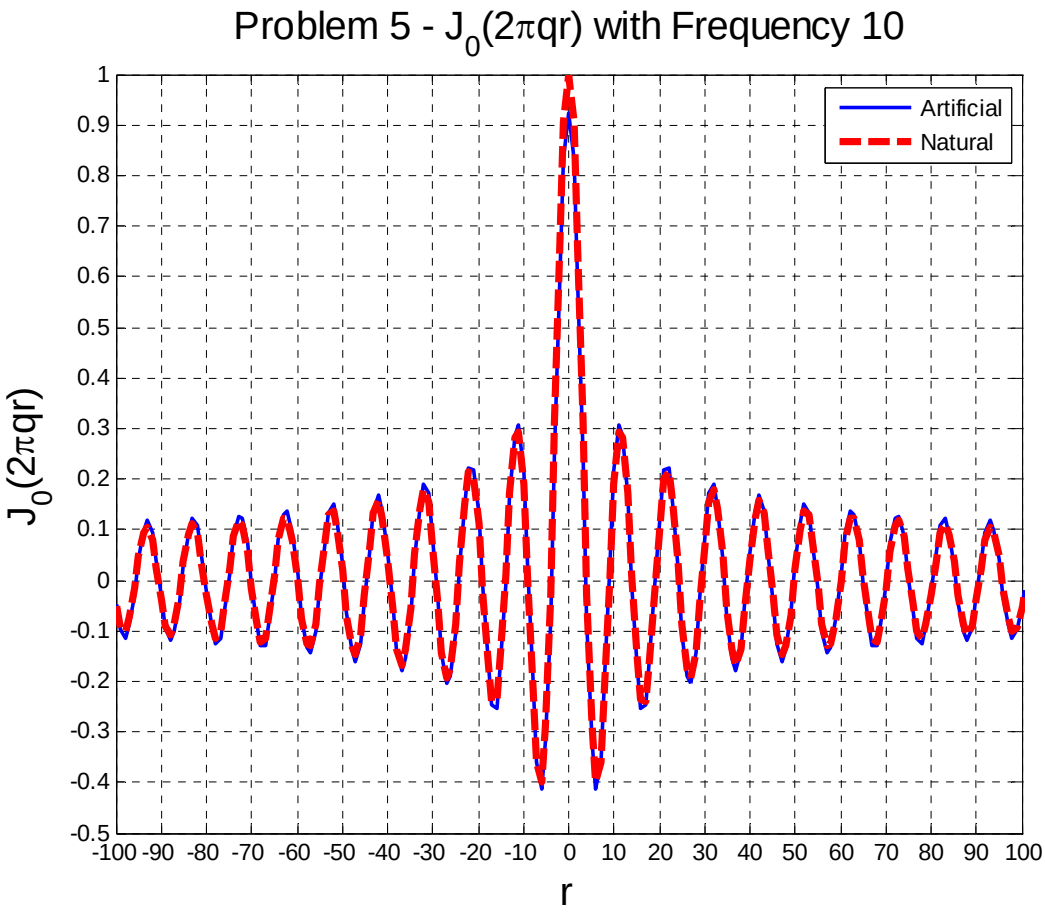
Problem 5 - J0(2πqr) with Frequency 10
Artificial
Natural
J0(2πqr)
r
1
0.9
0.8
0.7
0.6
0.5
0.4
0.3
0.2
0.1
0
-0.1
-0.2
-0.3
-0.4
-0.5
-100 -90 -80 -70 -60 -50 -40 -30 -20 -10 0 10 20 30 40 50 60 70 80 90 100

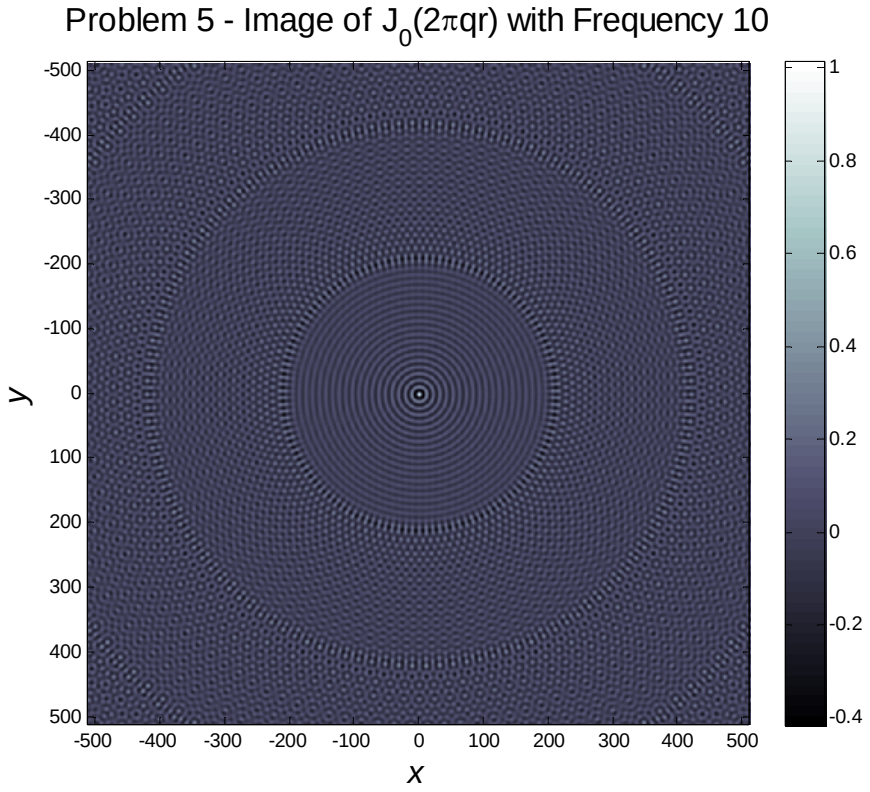
Problem 5 - Image of J0(2πqr) with Frequency 10
y
x
-500 -400 -300 -200 -100 0 100 200 300 400 500
1
0.8
0.6
0.4
0.2
0
-0.2
-0.4